Electronic Structure of Chromium Hexacarbonyl at Liquid Nitrogen Temperature. 2. Experimental Study (X-Ray and Neutron Diffraction) of σ and π Bonding

Bernard Rees* and André Mitschler

Contribution from the Laboratoire de Cristallochimie, Institut Le Bel, Université Louis Pasteur, 67070 Strasbourg-Cedex, France. *Received March 22, 1976*

Abstract: The charge density distribution in crystalline chromium hexacarbonyl was studied at liquid nitrogen temperature by x-ray and neutron diffraction (X-N method). The problem was simplified, and the precision enhanced, by assuming the chemical equivalence of the different Cr-C-O bonds and averaging over them. By spatial integration, the following atomic charges were obtained: Cr, 0.15 ± 0.12; C, 0.09 ± 0.05; O, -0.12 ± 0.05. The asphericity of the density around the chromium nucleus shows that 25% of the d electrons occupy the orbitals belonging to the representation e_g of the symmetry group O_h and 75% the orbitals belonging to the representation t_{2g}. Comparison of the carbonyl region with the density calculated from the Hartree-Fock wave function of carbon monoxide enables a direct visualization of the classical scheme of σ bonding and π backbonding with incomplete occupation of the π^* orbitals of CO. The σ or π electron transfer is 0.3 ± 0.1 electron per CO.

Chromium hexacarbonyl has been chosen as one of the most fundamental examples of the transition-metal carbonyls. Its electronic structure has generated great interest, as is attested by the number of molecular orbital calculations performed on this system,[1-10] with methods ranging from the semiempirical self consistent charge and configuration (SCCC) method[2-7] to an ab initio Hartree-Fock calculation.[8] Not surprisingly, there is considerable disagreement between the corresponding results. For example, the values obtained for the metal charge range from -1.0[1] to 1.8.[9] There is some lack of experimental evidence on the actual charge distribution in the molecule, although some experiments have given partial information: electronic spectra,[2] photoelectron spectra,[11-13] vibrational spectra, and determination of force constants.[9,14-16] However the interpretation of experimental data is often open to controversy, for example, as to the amount of electron transfer from the carbonyl ligands to the metal (σ bonds) and back from the metal to the carbonyls (π bonds).[17,18]

It seemed worthwhile, therefore, to attempt a direct study of the charge density distribution in crystalline $Cr(CO)_6$ by the method of precise x-ray and neutron diffraction analysis (the so-called X-N method). The neutron diffraction experiment and its results have been described in a preceding paper.[19] The present publication is devoted to the analysis of x-ray diffraction data, with the aid of the information on the positional and thermal parameters of the nuclei, obtained from neutron diffraction.

Experimental Section

X-Ray Data Collection and Processing. Details relative to the experimental conditions and the data processing are given in Table I.

A crystal, grown by sublimation, was cut into a sphere of 0.20 ± 0.01 mm diameter and sealed in a Lindeman glass capillary to avoid further sublimation. Low-temperature x-ray diffraction data were collected on a Picker diffractometer, equipped with a beryllium cryostat.[20] The initial equipment did not allow the crystal to be kept geometrically centered within better than 0.3 mm, as was shown by a comparison of the χ angles corresponding to the 2θ and -2θ positions of the detector (see ref 21, p 282). Considering the narrow x-ray beam profile due to the graphite monochromator,[20] such an imprecision is not compatible with the requirements of precise measurements. As a solution, the suppression of the monochromator has been proposed.[20] We chose to keep the monochromator and improve the precision by strengthening the goniometer head and removing most of the causes of mechanical strain. At the end of these modifications, the mechanical precision was improved by a factor of 10, so that the loss in diffracted intensity due to miscentering is always less than 1%. Liquid nitrogen was used as the cryogen, the circulation being insured by pumping. The temperature was 74 K, 4 deg lower than the temperature of the neutron experiment. The reason for this difference is the following: the cell dimensions determined in the x-ray experiment were about 0.1% larger than the corresponding values measured in the neutron experiment. This was interpreted as an indication that the effective crystal temperature during the neutron data collection (where cooling was insured by liquid helium) was lower than the measured value of 78 K, so the temperature during the x-ray experiment was kept as low as possible with liquid nitrogen. The least-squares refinements of the temperature factors (see below) showed later that the difference in the cell parameters had another origin, perhaps a slightly incorrect value of the neutron wavelength.

The data collection was split into two parts: (a) the measurement of "low-order" reflections, up to 65° in 2θ, which was done with special care: at least four symmetry equivalents were measured for each reflection, and the lowest-lying reflections were measured again with a smaller $\theta/2\theta$ speed (this was done to check the influence of the scan rate on the accuracy; it was concluded that the improvement with the lower speed was hardly significant); (b) the measurement of "high-order" reflections, up to 100° in 2θ, was conducted mainly to determine the nuclear positional and thermal parameters, and thus to supplement the neutron-diffraction data. Two symmetry equivalents were measured for each reflection.

Three reflections were used for monitoring purposes and recorded after every 60 measurements. No systematic variation of intensity was detected, except toward the end of the data collection, where a slight drop in intensity was noted, and corrected by a scaling procedure. The short-range fluctuations were found to be larger than what could be expected from the standard deviations, σ_{count}, calculated for a Poisson distribution, and became especially large for values of χ near 90°. The total variance could be expressed adequately by an empirical relation of the type:

$$\sigma^2(I) = \sigma_{count}^2 + p^2I^2 + q^2(\sin^2\chi)I^2$$

where I is the integrated intensity, and $p = 0.008$, $q = 0.027$. This relation was used to weight the individual measurements in an averaging procedure. The spread of symmetry-related reflections showed that $\sigma^2(I)$, determined as it was from the repeated measurement of the same reflection, was slightly underestimated and that the best estimate of the variance of the weighted-average intensity was:

$$\sigma^2(\bar{I}) = 1/\sum w_i + 0.015^2 \sum w_i^2 I_i^2/(\sum w_i)^2$$

where w_i is the inverse of $\sigma^2(I)$ calculated as above and the summations are carried over the symmetry-related reflections.

After correction for Lorenz and polarization effects, the diffracted intensities were also corrected for absorption, although this is small and fairly constant. The transmission factor and the mean absorption-weighted path length $\bar{T}$ (necessary for extinction corrections) were calculated for each reflection by numerical integration over a polyhedron of 26 faces having the same volume as the spherical crystal. The values of the transmission factor agree to within 0.04% with those

Table I. X-Ray Diffraction. Data Collection and Processing

Crystal: Space group: *Pnma*, $Z = 4$
$a = 11.505$ (4), $b = 10.916$ (3), $c = 6.203$ (2) Å
Crystal diameter: 0.20 ± 0.01 mm
Radiation: Mo Kα, $\lambda_{K\alpha_1} = 0.70930$ Å
Absorption: Linear absorption coefficient: $\mu = 15.27$ cm^{-1}
Transmission factor: 0.789–0.793
Cryostat transmission factor: 0.920–0.931
Data collection:
Takeoff angle: 1.2°
Monochromator: graphite
Mode: $\omega/2\theta$ scan (continuous)
Scanning interval, in 2θ: 1.8° + $\alpha_1\alpha_2$ splitting
Scanning speed in 2θ: 2°/min (except for 1328 reflections with $2\theta < 38°$, also measured at 1°/min)
Background determination: during 20 s at each end of the interval

	Low order ($2\theta < 65°$)	High order ($2\theta > 65°$)
Number of measurements (not including standard reflections)	8075	5015
Averaging		
Number of reflections after averaging	1482	2645
$\Sigma Av(\lvert I - Av(I)\rvert)/\Sigma Av(I)$	0.027	0.093
Least-squares refinement. All reflections included		
$R = \Sigma\lvert\lvert F_{obsd}\rvert - \lvert F_{calcd}\rvert\rvert/\Sigma\lvert F_{obsd}\rvert$	0.030	0.107
$R_w(F^2) = \{\Sigma w(\lvert F_{obsd}\rvert^2 - \lvert F_{calcd}\rvert^2)^2/\Sigma w\lvert F_{obsd}\rvert^4\}^{1/2}$	0.049	0.106
$S(F^2) = \{\Sigma w(\lvert F_{obsd}\rvert^2 - \lvert F_{calcd}\rvert^2)^2/(N_{obsd} - N_{par})\}^{1/2}$	2.56	1.22
Scale factor	2.212 (3)	2.181 (10)

Extinction: Weighted path length $\bar{T}$: 0.147–0.154 mm
Type assumed: secondary isotropic extinction, mosaic-spread dominated, Lorentzian distribution
Extinction parameter $g = 0.38\ (3) \times 10^4$ (mosaic spread: 15″)
Largest extinction (reflection 200): $y = 0.85$

published by Dwiggins for a spherical crystal.[22] A correction for the absorption of the x-ray beams by the cylindrical beryllium walls of the cryostat was also made. The occurrence of multiple reflection was checked with the program MULREF.[23] This check indicated a number of reflections which could be affected by multiple reflection, but comparison with their symmetry equivalents, and with the intensities calculated after completion of the crystal structure refinements, showed no evidence of extra error in the observed intensities.

The structure factors F_{calcd} were calculated for the usual model of noninteracting neutral spherical atoms in their ground state (hereafter called the free-atom model). Anomalous dispersion was allowed for all atoms.[21] The scattering factors were taken from Table 2.2A in ref 21, thus assuming a $3d^54s^1(^7S)$ configuration of chromium, as in the free atom. When needed, the scattering factor for the $3d^6(^5D)$ configuration was also considered.[24] The relativistic correction is neglected in this calculation, but it was assumed to be the same as for the $3d^54s^1$ configuration and estimated from the comparison of Tables 2.2A and 2.2B of ref 21 (respectively, with and without relativistic effects). Conventional least-squares refinements were performed separately for the two classes of data by minimization of $\Sigma w(F_{obsd}^2 - \lvert kF_{calcd}\rvert^2)$,[2] where F_{obsd}^2 and $w^{-1} = \sigma^2(F_{obsd}^2)$ are the corrected average intensity and its variance, estimated as described above; k is a scale factor. Figures of merit are given in Table I. The standard deviation of an observation of unit weight, $S(F^2)$, is near to one for the high-order data, which shows that the assumed model is approximately correct, but much larger for the low-order data: this indicates that the real crystal differs significantly from the free-atom model in the outer shells of the atoms. The relatively large values of the R factors for high-order data is simply due to the large number of very weak reflections, which are often considered as unobserved, but are all included here in the refinement.[25] Note that if the refinements were performed on F instead of F^2, the R_w factor would be divided by two. As a check of the overall accuracy of the data, a conventional refinement with all observed intensities larger than three times the estimated standard deviation (thus including 84% of the low-order and 63% of the high-order reflections) was performed. The agreement factors are the following: $R(F) = 0.038$; $R_w(F^2) = 0.055$; $R_w(F) = 0.029$.

Table III. Bond Lengths and Angles (uncorrected) from High-Order X-Ray Data and Neutron Data[19]

	Neutron	X-ray
Cr-C(1)	1.9132 (18) Å	1.9116 (19) Å
Cr-C (2)	1.9105 (18)	1.9160 (20)
Cr-C (3)	1.9125 (13)	1.9147 (13)
Cr-C (4)	1.9185 (13)	1.9180 (13)
C(1)-O(1)	1.1396 (14)	1.1426 (26)
C(2)-O(2)	1.1414 (14)	1.1411 (28)
C(3)-O(3)	1.1406 (10)	1.1390 (19)
C(4)-O(4)	1.1379 (10)	1.1380 (19)
Cr-C(1)-O(1)	180.00 (10)°	179.92 (22)°
Cr-C(2)-O(2)	179.46 (11)	179.05 (21)
Cr-C(3)-O(3)	179.37 (8)	179.37 (15)
Cr-C(4)-O (4)	179.10 (7)	179.20 (14)
C(1)-Cr-C(3)	90.34 (6)	90.37 (6)
C(1)-Cr-C(4)	89.96 (6)	90.14 (7)
C(2)-Cr-C(3)	90.06 (6)	89.94 (6)
C(2)-Cr-C(4)	89.65 (6)	89.55 (6)
C(3)-Cr-C(4)	89.79 (3)	89.85 (5)
C(3)-Cr-C (3a)	89.53 (8)	89.40 (8)
C(4)-Cr-C (4a)	90.89 (8)	90.89 (8)
C(1)-Cr-C(2)	179.44 (10)	179.56 (10)
C(3)-Cr-C (4a)	179.26 (8)	179.10 (6)

The positional and thermal parameters obtained from the refinement of the high-order data are given in Table II. The values of the same parameters obtained from the low-order data will not be discussed, since they may be more affected by bonding effects. However, none of the atomic coordinates differed by more than twice the estimated standard deviation. The thermal parameters, especially of the oxygen atoms, show the expected systematic differences due to electron concentration on the bond axes. In Table III, the bond lengths and valence angles from high-order x-ray data are compared to the corresponding values from neutron data.[19] The differences are never larger than twice their esd. The mean square amplitudes U of thermal motion from x-ray data are systematically lower than the values obtained from the neutron data. For the y and z directions this may be

Table II. Relative Coordinates (×10^5) and Mean Square Vibrational Amplitudes (in units of 10^{-4} Å^2) from High-Order X-Ray Data (the temperature factor is $\exp(-2\pi^2\Sigma\Sigma U_{ij}a_i^*a_j^*)$)

	x	y	z	U_{11}	U_{22}	U_{33}	U_{12}	U_{13}	U_{23}
Cr	12 748 (3)	25 000	6 182 (4)	68 (1)	61 (1)	67 (1)	0	0 (1)	0
C(1)	21 894 (19)	25 000	31 909 (28)	98 (6)	119 (5)	89 (4)	0	−8 (4)	0
C(2)	3 688 (20)	25 000	−19 735 (30)	98 (6)	123 (5)	96 (4)	0	−3 (4)	0
C(3)	2 814 (13)	37 338 (11)	18 091 (21)	100 (5)	95 (5)	107 (3)	14 (3)	10 (3)	−4 (3)
C(4)	22 491 (12)	37 520 (10)	−5 822 (25)	102 (4)	95 (3)	118 (3)	−8 (2)	5 (3)	16 (3)
O(1)	27 372 (23)	25 000	47 273 (30)	149 (8)	215 (7)	113 (4)	0	−46 (4)	0
O(2)	−1 570 (22)	25 000	−35 334 (31)	143 (7)	209 (6)	115 (4)	0	−41 (4)	0
O(3)	−3 167 (17)	44 660 (13)	25 025 (24)	155 (6)	136 (4)	172 (4)	57 (3)	29 (3)	−15 (3)
O(4)	28 164 (16)	45 040 (14)	−12 945 (26)	151 (5)	138 (4)	199 (5)	−45 (3)	13 (4)	52 (3)

Table IV. "Best" Positional ($\times 10^5$) and Thermal ($\times 10^4$) Parameters of $Cr(CO)_6$ (see text)

	x	y	z	U_{11}	U_{22}	U_{33}	U_{12}	U_{13}	U_{23}
Cr	12 748	25 000	6 182	68	61	67	0	0	0
C(1)	21 895	25 000	31 888	100	123	91	0	−10	0
C(2)	3 715	25 000	−19 712	102	122	99	0	−19	0
C(3)	2 828	37 337	18 065	107	95	113	10	4	−3
C(4)	22 499	37 524	−5 790	99	98	120	−11	3	16
O(1)	27 354	25 000	47 218	143	213	111	0	−43	0
O(2)	−1 593	25 000	−35 257	158	210	105	0	−47	0
O(3)	−3 157	44 662	25 042	147	129	183	55	25	−24
O(4)	28 167	45 041	−12 931	137	146	202	−39	15	54

Table V. Description of Thermal Motion from the Nuclear Thermal Parameters of Table IV[a]

Bond	$U_{z,Cr}$	$U_{z,C}$	$U_{z,O}$	$U_{x,C}$	$U_{x,O}$	ω_C	ω_O
Cr-C(1)-O(1)	0.0068	0.0084	0.0081	0.0115	0.0193	2.14	2.14
Cr-C(2)-O(2)	0.0068	0.0083	0.0078	0.0120	0.0198	2.24	2.17
Cr-C(3)-O(3)	0.0064	0.0090	0.0073	0.0112	0.0193	2.03	2.12
Cr-C(4)-O(4)	0.0064	0.0083	0.0082	0.0117	0.0201	2.14	2.18
Average	0.0065	0.0085	0.0078	0.0116	0.0196	2.12	2.15

[a] Mean square amplitudes are given in Å^2, in the direction of the bond (U_z) and in a perpendicular direction (U_x). ω_C and ω_O are the root mean square angular amplitudes of riding motion around Cr, in degrees.

accounted for by the difference in temperature (see above): in fact the differences agree fairly well with a linear dependence of the U's on the absolute temperature. The differences are larger in the x direction. This is probably related to the anomalies observed for a few neutron reflections with large values of h.[19] For those reasons, the neutron temperature factors were scaled to the high-order x-ray temperature factors, multiplying each U_{ij} by $\sqrt{k_i k_j}$, where $k_i = \Sigma U_{ii}(\text{x-ray})/\Sigma U_{ii}(\text{neutron})$. The values $k_1 = 0.864$, $k_2 = k_3 = 0.936$ were obtained. Furthermore, the comparison of the esd's shows that the high-order x-ray values of the parameters of chromium are much more accurate than the corresponding neutron values (this is due to the relatively small neutron scattering length of chromium) and, since they are not likely to be much affected by bonding, they were taken instead of the neutron values. These "best" nuclear parameters are given in Table IV.

Table V summarizes the corresponding analysis of thermal motion, which is seen to be essentially the same in all Cr-C-O directions. An extra rigid-body motion along the crystal a axis is no longer evident.[19] The motion may be decomposed into (a) rigid-body translational vibrations, which are essentially isotropic (mean square amplitude 0.0065 Å^2, corresponding to a B factor of 0.52 Å^2); (b) an extra translational motion of the carbonyl ligands along the bond axis; (c) a riding motion of the carbonyls around Cr. A stretching vibration of small amplitude of the carbonyls may account for the slight difference between the amplitudes of C and O along the bond.

Computing Programs. Most standard programs were local versions of programs originating from the Brookhaven National Laboratory and from the State University of New York at Buffalo: DATAP (data processing), SORT (sorting and averaging), LINEX (least-squares refinement with extinction corrections as derived by Becker and Coppens[26]), JIMDAP and FOURSEC (electron density calculation and plotting), ORFFE (bond lengths and angles).

Results and Discussion

Deformation Electron Density. The deformation electron density $\Delta\rho$ is defined as the difference between the true electron density in the crystal and the free-atom model, with the same instantaneous distribution of the nuclei. Experimentally, it is determined as the Fourier transform of $F_{obsd}/k - F_{calcd}$. F_{calcd} is calculated with the spherical free atom form factors, not affected by anomalous dispersion, and F_{obsd} is corrected for anomalous dispersion.[27] The nuclear parameters employed in the calculation of F_{calcd} were taken from Table IV.

This calculation, and those which follow, were limited to the "low-order" reflections ($(\sin\theta)/\lambda < 0.76$ Å^{-1}). It should therefore be emphasized that the electron density under discussion is the density "seen" with the limited resolution $\lambda/(2 \sin\theta_{max}) = 0.66$ Å. For this resolution, the average esd of the observed density, at some distance from the crystal symmetry elements, is 0.057 e Å^{-3}.

A value of 2.204 was obtained for the scale factor k by scaling the low-order observed structure factors F_{obsd} to the factors F_{calcd}, calculated with the positional and thermal parameters of Table IV. To avoid a systematic error due to the neglect of bonding characteristics, a "molecular model", discussed below, was considered in this calculation. This includes most of the atomic asphericity. However, when compared with the value obtained from the usual free-atom model, the change in k is only 0.02%, which shows a relative insensitivity to an explicit consideration of bonding details. Another source of systematic error could be the uncertainty in the atomic scattering factors, especially of chromium, or a bias in the nuclear parameters: since the scattering from the outer shells of chromium extends far into the reciprocal space (see below), the temperature parameters of this atom, determined as they are from the high-order x-ray data, could be sensitive to the assumed configuration. In an attempt to estimate the limits of this error, the high-order refinement and the scaling procedure of the low-order data were repeated with the chromium $3d^6$ instead of $3d^54s^1$ scattering factor. The change in the temperature factors was less than 0.2 times the esd's, and the final change in k only 0.05%. A large systematic error in the scale factor, due to the electron distribution, is therefore not likely.

A section of the deformation density is shown in Figure 1. The same general features of the deformation density are observed in the four Cr-C-O directions shown. The differences are generally less than twice their esd,[28] except between the carbon lone pair regions of atoms C(1) and C(3), which differ by three times the esd. It is possible to improve the precision in the experimental electron density if chemical equivalence of all the carbonyls is assumed. This seems justified, since the $Cr(CO)_6$ octahedron is almost regular. Although some small significant deformations are observed, they are not likely to alter significantly the electron density. This regularity is not only observed for the geometrical parameters, but also for the thermal motion (see Table V). Moreover, the interactions with

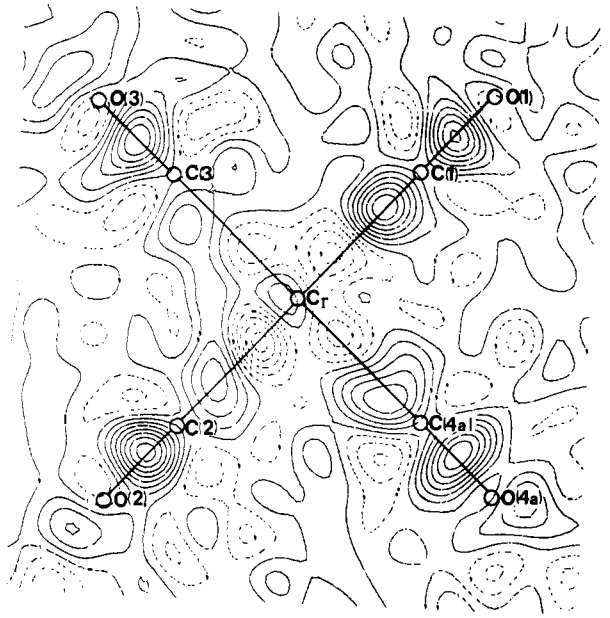

Figure 1. Section of the electron deformation density (observed density minus free-atom model) at 0.66-Å resolution ($(\sin\theta_{max})/\lambda = 0.76$ Å^{-1}). The plane passes near the nuclei of all nine crystallographically independent atoms. Contour interval: 0.1 e Å^{-3}. Zero and positive contours are represented by solid lines, negative contours by dashed lines.

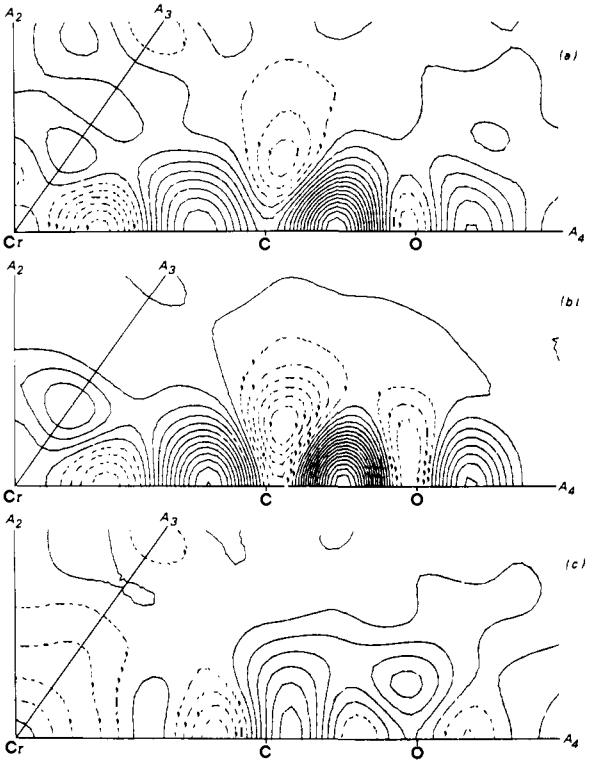

Figure 2. (a) Average deformation density (observed density minus free atoms). (b) Calculated deformation density: molecular model (chromium in configuration $3d(t_{2g})^{3.8}3d(e_g)^{1.2}4s$ + carbon monoxide molecules) minus free atoms. (c) Average observed density minus molecular model. A_2, A_3, and A_4 represent, respectively, two-, three-, and fourfold axes in the idealized octahedron. Same resolution as in Figure 1. Contour interval: 0.05 eÅ^{-3}.

the neighboring molecules are small and the surroundings roughly isotropic.[19] The averaging procedure, with a weighting scheme which depends on the estimated variances and covariances of $\Delta\rho$ at the equivalent points, has been described elsewhere.[28] The result for the plane containing one Cr–C–O bond and bisecting two other bonds is shown on Figure 2a. Each general point in this plane results from the averaging over 14 chemical equivalents (ten in the general position and four in the mirror plane). The validity of the assumption of chemical equivalence and the correctness of the estimation of the standard deviations $\sigma(\Delta\rho)$ may be checked by comparing to one the multiplying factor of $\sigma(\Delta\rho)$, given by

$$s = \left\{ \left(\sum_{i=1}^{m} \sum_{j=1}^{m} \Delta\rho_i \Delta\rho_j P_{ij} - \overline{\Delta\rho^2} \sum_{i=1}^{m} \sum_{j=1}^{m} P_{ij} \right) \Big/ (m-1) \right\}^{1/2}$$

where m is the number of equivalent points and **P** the inverse of the estimated variance–covariance matrix.[28] The root-mean-square value of s is 1.18 for the planes considered. A map of the esd $\sigma(\overline{\Delta\rho})$ has been given in ref 28: σ is less than 0.02 e Å^{-3} at some distance from the symmetry elements of the regular octahedron, but, due to the imprecision of the nuclear parameters, it becomes large in the vicinity of the nuclei: 0.27 e Å^{-3} at Cr, 0.08 at C, 0.10 at O (not including the error in the scale factor).

Integrated Atomic Charges. Various definitions have been given of the atomic charges in a molecule. They are all necessarily arbitrary, as the concept of atoms in a molecule is itself ill-defined. In a spatial definition, the molecule is divided into nonoverlapping volumes, each of which belongs to one atom. The charge of the atom is determined by integration of the electron density over this atomic volume. The atomic volumes may be simply limited by planes perpendicular to the internuclear vectors. To determine the position of these planes, the condition may be imposed that the atoms be neutral in the free-atom model: integration of the calculated density (at the same resolution as the deformation density, but obtained from the factors F_{calcd}) should yield the nuclear charges Z.

The calculation was first done by numerical integration of the average deformation density, over points distant by no more than 4.2 Å from the Cr nucleus and 1.5 Å from the bond axes. Cr, C, and O were separated by planes at 1.0 and 2.55 Å from the Cr nucleus. The results are in electron units: Cr, 0.15; C, 0.09; O, −0.12.

An alternative method is the use of the equations given by Coppens and Hamilton[29] for charge integration over a parallelepiped, by summation in reciprocal space. This has the advantage of enabling an estimation of the standard error (the formulas were adapted to the space group *Pnma*). Integration was performed over two cubes centered on Cr, and so chosen as to contain $Z(Cr) = 24$ and $Z(Cr) + 6Z(C) = 60$ electrons, respectively, when the factors F_{calcd} of the low-order reflections are used in the summations. The charges were obtained by summation over $F_{obsd}/k - F_{calcd}$, for the same reflections. The position of the limiting planes was slightly different from the result of numerical integration (0.95 and 2.26 Å), but the charges of Cr and C were the same. The standard errors due to imprecision in the observed structure factors are 0.036 and 0.016 for Cr and C. The imprecision in the scale factor contributes 0.02 and 0.03, respectively. The error due to the choice of the atomic volumes is of course more difficult to estimate. However, if the planes are displaced by 0.1 Å, the calculated number of electrons in the atomic volume of chromium as well as in the atomic volume of one carbon changes by approximately one and the charges by 0.05 and 0.03, respectively. The following error intervals seem thus resonable limits:

$$\text{Cr, } 0.15 \pm 0.12\text{; C, } 0.09 \pm 0.05\text{; O, } -0.12 \pm 0.05$$

The interesting point about these atomic charges is their small absolute value, which is in agreement with the electroneutrality principle, but in contrast to the quantum chemical calculations. The comparison is made in Table VI, for the most recent calculations only. Of course, one must keep in mind that the definition of the atomic charge is not the same: the method of space partition used here, although it suffers from some

Table VI. Charge and Configuration in $Cr(CO)_6$. Comparison with Recent Quantum-Chemical Calculations

Ref	Method	q_{Cr}	q_C	q_O	Shell 4 occupation	% 3d(e_g)[b]	Transfer σ	Transfer π
7	SCCC	0.28			0.49	4	0.11	0.15
10	Extended CNDO	0.50	0.04	−0.12	0.71	15	0.26	0.35
9	DVXα	1.80	0.05	−0.35	−0.10	26	0.23	0.53
8	SCF ab initio	0.70	0.23	−0.35	−0.23	16	0.16	0.27
This work	Experimental	0.15 ± 0.12	0.09 ± 0.05	−0.12 ± 0.05	1[a]	24 ± 3	0.35 ± 0.04	0.38 ± 0.04
					0[a]	25 ± 3	0.24 ± 0.04	0.27 ± 0.04

[a] Assumed. [b] 100 × (number of electrons in $3d_{z^2}$ and $3d_{x^2-y^2}$)/(number of 3d electrons). This is 40% in spherical chromium.

arbitrariness too, is probably sounder than the Mulliken definition used generally in theoretical work, which divides equally the overlap populations between bonded atoms. Disagreement is also found between the present results and the atomic charges derived from other experimental data: 0.4 electron on chromium from x-ray absorption measurements;[30] −0.55 or 1.27 (due to some sign ambiguity) from infrared spectra.[16]

Configuration of Chromium. The interesting feature of the electron density around the chromium nucleus (Figure 2a) is its lack of spherical symmetry: the deformation density is largest in the direction of the threefold axes (A_3) of the idealized octahedron and lowest in the direction of the bonds (fourfold axes A_4). Analogous features were observed in benzenechromium tricarbonyl,[31] in $[Co(NH_3)_6][Co(CN)_6]$,[32] and in γ-Ni_2SiO_4.[33]

Due to the symmetry of the idealized octahedron, the electron density of the p orbitals of chromium has spherical symmetry, as do the s orbitals. At a short distance from the chromium nucleus, where the value of the carbonyl orbitals is negligible, asymmetry can arise only from the 3d orbitals (or 4d, 4f, . . . , which are too high in energy to play an important role). In the O_h symmetry group, the d orbitals fall into two representations: d_{xy}, d_{yz}, and d_{zx} in t_{2g}; d_{z^2} and $d_{x^2-y^2}$ in e_g. Let us write the configuration of chromium as [Ar]3d-$(t_{2g})^{3m}$3d$(e_g)^{2n}$4s^q. Thus, in the free Cr atom: $m = n = q = 1$. The contribution of the 4p orbitals is not considered explicitly here, but this is unimportant, as q may be defined as the total occupancy of shell 4 as well.

It is unfortunately almost impossible to determine experimentally the occupancy of shell 4, as is seen when the spherically averaged electron density is calculated for both configuration $3d^54s^1$ and $3d^6$. With the experimental temperature factor (B = 0.52 Å^2) and the actual resolution (0.66 Å), the difference is 0.16 e Å^{-3} at the nucleus (compared to a total density of 120 e Å^{-3}) and becomes smaller as the distance to the nucleus increases, until a minimum of −0.10 e Å^{-3} is reached at 0.6 Å. Such differences are too small and the experimental deformation density around Cr depends on too many parameters (form factor, temperature factor, scale factor) for the determination of the occupancy q to be possible. The two configurations $3d^54s^1$ and $3d^6$ may be considered as limits, with the actual configuration probably in between.

For an assumed value of q, it is possible to determine the populations m and n of the d orbitals from the asphericity of the electron density around chromium. The total scattering of the 3d orbitals (without thermal motion) is:[34]

$$f(3d) = (3m + 2n)\langle j_0\rangle + 3(n - m)A(\mathbf{H})\langle j_4\rangle$$

with $A(\mathbf{H}) = [(h^2 + k^2 + l^2)^2 - 5(h^2k^2 + k^2l^2 + l^2h^2)]/(h^2 + k^2 + l^2)$, where h, k, and l are Miller indices in a cubic lattice. $\langle j_0\rangle$ and $\langle j_4\rangle$ are tabulated.[21,24] The Fourier transform of $A(\mathbf{H})\langle j_4\rangle$ is proportional to the aspherical part of the electron density. The asphericity may be characterized by the difference $\Delta\rho_a$ between this function in the directions of the fourfold and the threefold axes:

$$\Delta\rho_a = [\rho(A_3) - \rho(A_4)]/[3(m - n)]$$

Figure 3 shows the result of theoretical calculations of $\Delta\rho_a$ for various temperatures and resolutions, assuming configuration $3d^54s^1$. The position of the peak depends mainly on the resolution, while its height is dependent on both resolution and temperature. At the 0.66-Å resolution there is a gain of a factor of 2 in going down from room temperature to liquid nitrogen temperature. The two factors cannot be considered separately:

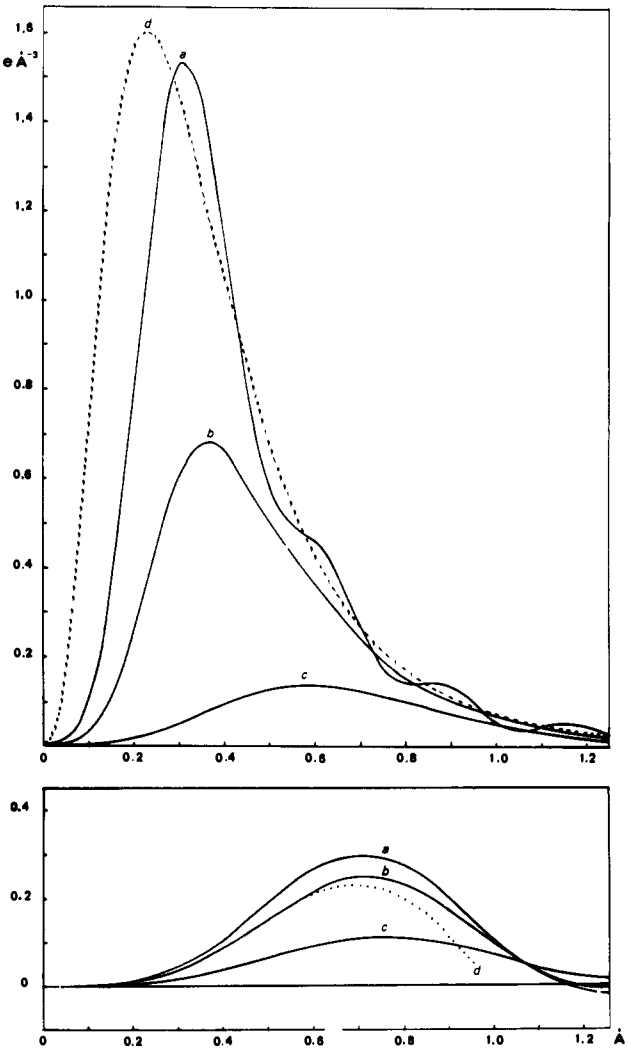

Figure 3. Calculated asphericity function of chromium $\Delta\rho_a = [\rho(A_3) - \rho(A_4)]/(3m - 3n)$ vs. distance from the nucleus. m and n are the occupancies of a 3d(t_{2g}) and a 3d(e_g) orbital, respectively: above, resolution = 0.26 Å ($(\sin\theta_{max})/\lambda$ = 1.9 Å^{-1}); below, resolution = 0.66 Å; a, no thermal motion; b, B = 0.516 Å^2 (T = 74 K); c, B = 2.70 Å^2 (room temperature[40]). The dashed curve d (above) represents the asphericity function calculated directly from the Hartree-Fock atomic orbitals.[41] The dotted curve d (below) is the experimental curve $[\rho_{obsd}(A_3) - \rho_{obsd}(A_4)]/2.0$. For small distances this curve is indistinguishable from curve b.

it would be useless, for instance, to lower the temperature further unless the resolution could be improved, which means that precision in the high-order intensities should be improved first.

The experimental curve is shown on Figure 3 (dotted), scaled to the theoretical curve calculated for the actual thermal motion and resolution. With a proportionality factor $3(m - n) = 2.0$ (for the $3d^5 4s^1$ configuration), the two curves are practically coincident up to 0.6 Å from the Cr nucleus. For larger distances, the density of the carbonyl ligands becomes important and they diverge. Since only differences in electron density, in different directions but at the same distance from the nucleus, are considered here, there is practically no error due to the scale factor.[28] Imprecision is due only to $\sigma(\rho_{obsd})$. The standard deviation $\sigma[\rho_{obsd}(A_3) - \rho_{obsd}(A_4)]$ is 0.05 e Å^{-3}, which is about 10% of the maximum difference. The calculated curve has only two sources of error: the isotropic temperature factor B and the $\langle j_4 \rangle$ curve for Cr 3d electrons; it is independent of the form factor for the core electrons. From these considerations, a maximum relative error of 20% was assumed for the coefficient $m - n$.

If the configuration $3d^6$ is considered,[24] a value of 2.2 is obtained for $3(m - n)$. The percentage of d electrons belonging to the e_g representation is practically the same in both cases: 24 and 25%, respectively, with a maximum absolute error of 3%.

Molecular Model of the Electron Density. A better approximation to the electron density than the free-atom model is a model consisting in the juxtaposition of aspherical chromium and carbon monoxide molecules in their ground state, both with the same thermal motion as in crystalline $Cr(CO)_6$. Chromium was taken as neutral, but in a configuration which agrees with the observed asphericity: $3d(t_{2g})^{3.8}3d(e_g)^{1.2}4s^1$, or $3d(t_{2g})^{4.5}3d(e_g)^{1.5}$. The theoretical deformation density of free CO was obtained from the Hartree–Fock wave function of McLean and Yoshimine.[35,36] To take account of the thermal motion (B = 0.52 Å^2) and the experimental resolution, a double Fourier transformation was performed on the theoretical deformation density, $\Delta\rho$. It may be shown that, for rigid-body thermal motion, the Fourier transform of the density is

$$F(\mathbf{H}) = \int \Delta\rho(\mathbf{r}) T(\mathbf{H},\mathbf{r}) e^{2\pi i \mathbf{H}\cdot\mathbf{r}} \, d^3\mathbf{r}$$

If z is along the bond axis, the temperature factor for cylindrical symmetry is

$$T(\mathbf{H},\mathbf{r}) = \exp[-(h^2 + k^2)U_x(\mathbf{r}) - l^2 U_z(\mathbf{r})]$$

U_x and U_z were calculated from the analysis of thermal motion given above. Within this approximation, and insofar as the small riding motion can be assimilated to linear vibration, U_x does not depend on x and is linearly dependent on z^2. As a check, curvilinear motion was allowed in a calculation with the third-order cumulant of Pawley and Willis,[37] performed on oxygen: the maximum change in the calculated density was only 0.01 e Å^{-3}. To allow to some extent for the small difference between $U_{z,C}$ and $U_{z,O}$ resulting from the carbonyl stretching vibration, a linear variation of U_z between the C and O nuclei was assumed.

The Fourier transforms were calculated by numerical integration (Simpson's method) using the formulas for distributions of cylindrical symmetry.[38] Care was taken to ensure that the results did not suffer from insufficient integration limits over $\Delta\rho$ or an insufficient number of grid points.

The contribution of the difference between the molecular model and the free-atom model was added to the low-order factors, F_{calcd}, and the overall scale factor to F_{obsd} was determined at this stage, as stated above. The crystallographic R factor dropped from 0.030 to 0.024 (0.025 for the $3d^6$ configuration of chromium). Only six calculated structure factors (of very weak reflections, three of them even below the background) changed sign by this addition. These few signs have no effect on the deformation density and one may conclude that the free-atom model gives the correct values of the signs, at least in this particular case.

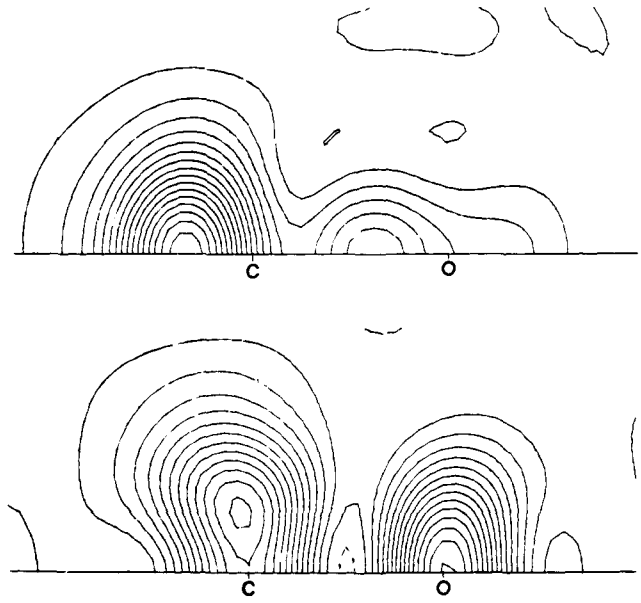

Figure 4. Dynamic electron density at 0.66-Å resolution for one electron in orbital 5σ (above) and 2π (or π^*, below) of carbon monoxide. Molecular orbitals are from ref 39. Thermal motion is as observed in $Cr(CO)_6$. Contour interval: 0.05 e Å^{-3}.

The difference between the molecular model ($3d^5 4s^1$ configuration) and the free-atom model is shown in Figure 2b. The map agrees qualitatively with the deformation density of Figure 2a. Figure 2c shows the difference between the two maps, i.e., the difference between the observed density ρ_{obsd} and the molecular model. The slightly negative zone (−0.1 e Å^{-3}) around chromium is not significant, for the reasons given above. Nevertheless it may be noted that if a $3d^6$ configuration is assumed for Cr, this residue becomes more negative, about −0.2 e Å^{-3}. More interesting are the quite significant residual features in the carbonyl region. For comparison, Figure 4 shows the squared amplitude of the orbitals 5σ and 2π (respectively, the highest occupied σ and the lowest virtual π orbitals) of carbon monoxide. The MO's are from a calculation by Nesbet, in a double ζ basis with d polarization function.[39] The densities were obtained, as before, by a double Fourier transformation and are for the same thermal motion and resolution as in $Cr(CO)_6$. The simple scheme of σ bonding and π backbonding would imply a lower occupation of 5σ in the complex than in free CO, compensated by a partial occupation of 2π. This is seen indeed on Figure 2c, which thus provides direct experimental evidence of the qualitative validity of this simple description of the bonding mechanism.

σ Bonding and π Backbonding. It is possible to obtain an approximate value of the σ and π "electron transfers". Since the charge of CO was found to be almost zero, the two transfers must be practically equal. The best agreement of Figure 2c with the molecular orbital densities of Figure 4 is obtained for an occupancy of 1.6 and 0.4 electrons of orbitals 5σ and 2π, respectively. The electron transfer (σ or π) would thus be about 0.4 electron per CO. This estimate is not very reliable, principally because of the approximations made in treating the thermal motion. Other sources of error are the inaccuracy of the wave function and the description of the bonding mechanism itself in the basis of the two functions 5σ and 2π, which is probably an oversimplification. It must also be noticed that

overlap with chromium has been implicitly neglected: orbital products like 3d(Cr) 5σ(CO), which make a nonnegligible contribution in the carbon lone-pair region, were not considered.

A more precise estimate may be obtained from the configuration of chromium, for which thermal motion can be more accurately taken into account. In the symmetry group O_h, there is an almost complete separation of σ and π bonding, except for the t_{1u} representation, which may mix σ orbitals of one carbonyl with π orbitals of another through the p orbitals of the metal. However, the p-π overlap is too small, compared to the p-σ overlap, to be of any real importance in the bonding. Thus the bonding orbitals of σ-type mix the σ orbitals of CO with the 3d(e_g) and the shell 4 orbitals of chromium, while the π orbitals involve the 3d(t_{2g}) orbitals of Cr and the π orbitals of CO. The σ-electron transfer may be characterized as well by the total occupancy of 3d(e_g), 4s, and 4p orbitals of the metal and the π transfer may be determined from the loss of occupancy of the 3d(t_{2g}) orbitals, compared to an "initial" occupancy of six. When the total charge of -0.03 on CO is taken into account, the σ and π transfers are 0.35 and 0.38 electron if a configuration $3d^5 4s^1$ is assumed, and about 0.1 electron less for a $3d^6$ configuration, with a maximum error of 0.04 electron in each case. These values are compared with MO calculations in Table VI. The former values are in excellent agreement with the value obtained from the inspection of the carbonyl regions. The final best estimate of electron transfers is

$$\text{transfer } \sigma \simeq \text{transfer } \pi \simeq 0.3 \pm 0.1 \text{ electron}$$

Conclusion

Although the assumption of a $3d^5 4s^1$ configuration of chromium leads to a slightly better internal consistency than a $3d^6$ configuration (smaller discrepancy between the two determinations of the electron transfer and lower residual features in the chromium region of Figure 2c), this cannot be considered as conclusive evidence for a partial occupancy of shell 4, which would contradict the most elaborate quantum chemical calculations.[8,9] The meaningful results obtained for the atomic charges, the relative occupancies of the two types of chromium 3d orbitals, and the amount of σ- and π-electron transfer, show that a study by diffraction methods of a simple transition-metal complex like chromium hexacarbonyl may be carried at a quantitative level. The electron configuration of the carbonyl ligands can be clearly distinguished from that of carbon monoxide and discussed on the basis of a simple molecular orbital theory.

Acknowledgment. Thanks are due to Dr. De With for communication of the Hartree-Fock electron deformation density of CO. We are grateful to Dr. Charles Burggraf: without his help in improving the mechanical stability of the cryogenic equipment, a precise low-temperature x-ray diffraction study would have been impossible.

Supplementary Material Available: A list of observed and calculated structure factors (17 pages). Ordering information is given on any current masthead page.

References and Notes

(1) K. G. Caulton and R. F. Fenske, *Inorg. Chem.*, 7, 1273–1284 (1968).
(2) H. B. Gray and N. A. Beach, *J. Am. Chem. Soc.*, **85**, 2922–2927 (1963); **90**, 5713–5721 (1968).
(3) D. G. Carroll and S. P. McGlynn, *Inorg. Chem.*, 7, 1285–1290 (1968).
(4) A. F. Schreiner and T. L. Brown, *J. Am. Chem. Soc.*, **90**, 3366–3374 (1968).
(5) D. A. Brown and R. M. Rawlinson, *J. Chem. Soc. A*, 1530–1534 (1969).
(6) I. H. Hillier, *J. Chem. Phys.*, **52**, 1948–1951 (1970).
(7) W. J. Chambers and N. J. Fitzpatrick, *Proc. R. Ir. Acad., Sect. B*, **71**, 97–108 (1971).
(8) I. H. Hillier and V. R. Saunders, *Mol. Phys.*, **22**, 1025–1034 (1971).
(9) E. J. Baerends and P. Ros, *Mol. Phys.*, **30**, 1735–1747 (1975).
(10) A. Serafini, M. Pelissier, J. M. Savariault, P. Cassoux, and J. F. Labarre, *Theor. Chim. Acta*, **39**, 229–239 (1975).
(11) J. A. Connor, M. B. Hall, I. H. Hillier, W. N. E. Meredith, M. Barber, and Q. Herd, *J. Chem. Soc., Faraday Trans. 2*, **69**, 1677–1684 (1973).
(12) B. R. Higginson, D. R. Lloyd, P. Burroughs, D. M. Gibson, and A. F. Orchard, *J. Chem. Soc., Faraday Trans. 2*, **69**, 1659–1668 (1973), and references cited therein.
(13) E. J. Baerends and P. Ros, *J. Electron Spectrosc.*, **7**, 69–74 (1975).
(14) L. H. Jones, R. S. McDowell, and M. Goldblatt, *Inorg. Chem.*, **8**, 2349–2363 (1969).
(15) A. Terzis and T. G. Spiro, *Inorg. Chem.*, **10**, 643–645 (1971).
(16) S. K. Samvelyan, V. T. Aleksanyan, and B. V. Lokshin, *J. Mol. Spectrosc.*, **48**, 47–56 (1973).
(17) F. A. Cotton, *Inorg. Chem.*, **3**, 702–711 (1964).
(18) G. R. Dobson, *Inorg. Chem.*, **4**, 1673–1675 (1965).
(19) A. Jost, B. Rees, and W. B. Yelon, *Acta Crystallogr., Sect. B*, **31**, 2649–2658 (1975). The *z* coordinate of O(1) (Table IV) should be 0.47218 (and not 0.47128).
(20) P. Coppens, F. K. Ross, R. M. Blessing, W. F. Cooper, F. K. Larsen, J. G. Leipoldt, B. Rees, and R. Leonard, *J. Appl. Crystallogr.*, **7**, 315–319 (1974).
(21) "International Tables of X-Ray Crystallography", Vol. IV, Kynoch Press, Birmingham, 1974.
(22) C. W. Dwiggins, Jr., *Acta Crystallogr., Sect. A*, **31**, 395–396 (1975).
(23) P. Coppens, *Acta Crystallogr., Sect. A*, **24**, 253–257 (1968).
(24) R. E. Watson and A. J. Freeman, *Acta Crystallogr.*, **14**, 27–37 (1961).
(25) F. L. Hirshfeld and D. Rabinovich, *Acta Crystallogr., Sect. A*, **29**, 510–513 (1973).
(26) P. J. Becker and P. Coppens, *Acta Crystallogr., Sect. A*, **30**, 129–147 (1974); **30**, 148–153 (1974); **31**, 417–425 (1975).
(27) J. A. Ibers and W. C. Hamilton, *Acta Crystallogr.*, 17, 781–782 (1964).
(28) B. Rees, *Acta Crystallogr., Sect. A*, **32**, 483–488 (1976).
(29) P. Coppens and W. C. Hamilton, *Acta Crystallogr., Sect. B*, **24**, 925–929 (1968).
(30) R. L. Barinskii and E. G. Nadzhakov, *Izv. Akad. Nauk SSSR, Ser. Fiz.*, **24**, 407–414 (1960).
(31) B. Rees and P. Coppens, *Acta Crystallogr., Sect. B*, **29**, 2516–2528 (1973).
(32) M. Iwata and Y. Saito, *Acta Crystallogr., Sect. B*, **29**, 822–832 (1973).
(33) F. Marumo, M. Isobe, Y. Saito, T. Yagi, and S. Akimoto, *Acta Crystallogr., Sect. B*, **30**, 1904–1906 (1974).
(34) R. J. Weiss and A. J. Freeman, *J. Phys. Chem. Solids*, **10**, 147–161 (1959).
(35) A. D. McLean and M. Yoshimine, "Tables of Linear Molecular Wave Functions", supplement to *IBM J. Res. Dev.*, 11 (Nov. 1967).
(36) G. De With and D. Feil, *Chem. Phys. Lett.*, **30**, 279–283 (1975).
(37) G. S. Pawley and B. T. M. Willis, *Acta Crystallogr., Sect. A*, **26**, 260–262 (1970).
(38) "International Tables of X-Ray Crystallography", Vol. II, Kynoch Press, Birmingham, 1959, p 72.
(39) R. K. Nesbet, *J. Chem. Phys.*, **40**, 3619–3633 (1964); **43**, 4403–4409 (1965).
(40) A. Whitaker and J. W. Jeffery, *Acta Crystallogr.*, **23**, 984–989 (1967).
(41) J. B. Mann, Los Alamos, Report Nb LA 3691; *At. Data Nucl. Data Tables*, **12**, 1–87 (1973).